Arrays of crystalline C_{60} and pentacene nanocolumns

Jian Zhang,[a] Ingo Salzmann, Siegfried Rogaschewski, Jürgen P. Rabe, and Norbert Koch[b]
Institut für Physik, Humboldt-Universität zu Berlin, Newtonstrasse 15, D-12489 Berlin, Germany

Fujun Zhang and Zheng Xu
Key Laboratory of Luminescence and Optical Information, Ministry of Education, Institute of Optoelectronic Technology, Beijing Jiaotong University, Beijing 100044, China

(Received 23 January 2007; accepted 18 April 2007; published online 9 May 2007)

Crystalline nanocolumn arrays of two organic semiconductors, C_{60} and pentacene, were fabricated by glancing angle deposition and characterized by scanning electron microscopy and x-ray diffraction. The diameter of the nanocolumns is typically 100 nm and essentially independent of column height (up to 360 nm for pentacene). The surface diffusion length of the molecules is identified as a key parameter for the formation of the nanocolumns. Our results indicate that glancing angle deposition is a simple technique to fabricate organic crystalline nanocolumn arrays, and controlling the surface diffusion via chemical and/or morphological patterning may lead to innovative organic nanostructures. © *2007 American Institute of Physics*.
[DOI: 10.1063/1.2738193]

Organized nanocolumns on large surface areas are important for obtaining scaled-up functional devices, such as sensors, field emitters, and nanoelectronic devices, in general. Significant efforts have been directed towards finding processes for the fabrication of inorganic nanocolumnar arrays, e.g., made of ZnO, InGaN/GaN, or metal nanorods.[1–3] An organic nanocolumn array based on carbon nanotubes[4,5] can, for instance, be used as sensor or catalyst because of its large surface area. However, only a few attempts to fabricate organic semiconductor nanocolumns have been made. Only recently Hrudey *et al.* have reported anisotropic optical properties for arrays made of the amorphous organic semiconducting material tris(8-hydroxyquinoline)aluminum.[6,7] The realization of crystalline nanocolumnar arrays of organic semiconductors can be seen as the next important step towards exploring new functionality of these materials. For example, combining such an array with another organic semiconductor could lead to highly efficient organic solar cells, since maximizing the interface-area between the two semiconductors in a columnar architecture should allow for optimal charge separation and transport.[8,9]

Glancing angle deposition (GLAD) comprises the combination of an oblique-angle incidence of the deposited material (on the substrate) and simultaneous substrate rotation, which leads to thin films with columnar structures on the nanometer scale in all three dimensions.[10,11] By changing the incidence angle [Fig. 1(a)], the columnar structure can be controlled through shadowing effects during island growth. Other parameters include the material itself, the deposition rate, the substrate temperature, and the substrate rotation rate.[12–14] In this letter, we report on the fabrication of crystalline nanocolumnar arrays of two widely studied organic semiconductors, i.e., fullerene (C_{60}) and pentacene [Fig. 1(b)], by GLAD. Substrates were Si wafer covered with native oxide and indium tin oxide (ITO), which represent the most widely used substrate materials in the field of organic electronics. We identify the surface diffusion length of the molecular material on the substrate as a general critical parameter for the realization of organic nanostructured arrays.

C_{60} and pentacene (purchased from Sigma-Aldrich) were evaporated onto oxidized Si and ITO substrates. Substrates were treated by standard solvent-cleaning procedures before use. Deposition was carried out in a custom vacuum chamber at a base pressure $<2\times10^{-4}$ Pa. Substrates were mounted on a substrate holder attached to a computer-controlled stepper motor that allowed sample rotation about the substrate normal. The oblique angle of the substrate relative to the incoming molecular flux was adjusted by a precision rotary motion feedthrough and set to 80° off the substrate normal. During deposition, the center of the substrate was 15 cm away from the evaporation sources. The film thickness and the deposition rate were monitored by a quartz-crystal microbalance. Deposition rates at the substrate surface were in the range of $1-3$ Å s^{-1}. The morphology of samples and substrates was studied using scanning electron microscopy (SEM) and atomic force microscopy (AFM). Prior to SEM imaging, samples were cleaved using a diamond scribe to facilitate cross-section viewing and coated with a thin Au film in order to avoid sample charging. X-ray diffraction experiments were performed at the synchrotron light source Hasylab (Hamburg) at beamline W1.

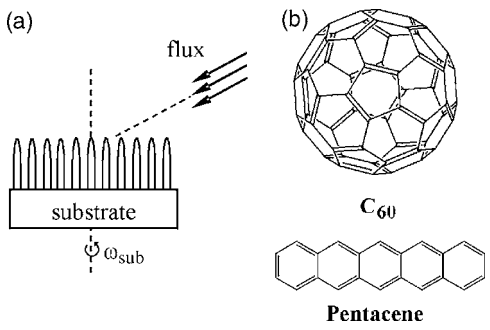

FIG. 1. (a) Schematic of glancing angle deposition. (b) Chemical structure of C_{60} and pentacene.

[a]Electronic mail: ciaczj@hotmail.com
[b]Electronic mail: norbert.koch@physik.hu-berlin.de

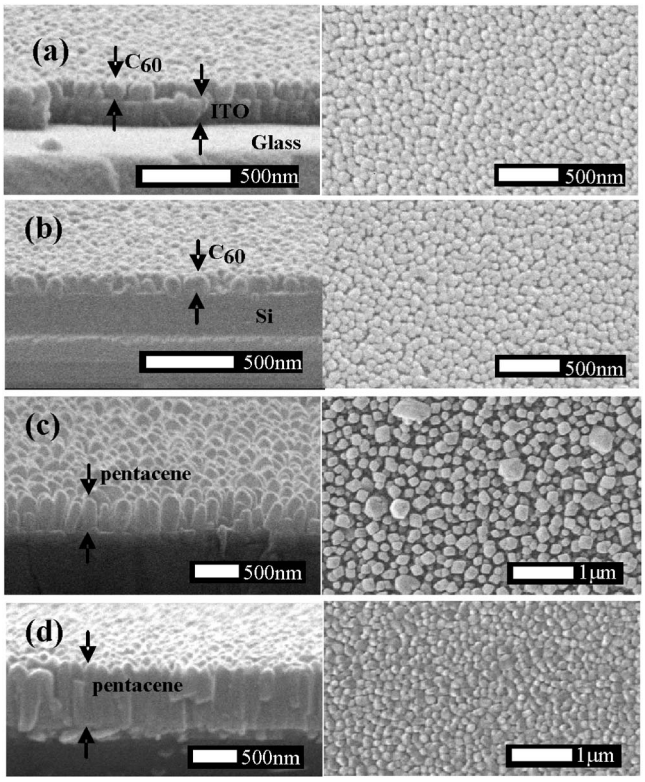

FIG. 2. SEM micrographs of C_{60} and pentacene films. (a) Section view (left) and top view (right) for C_{60} nanocolumn array on ITO. (b) Section view (left) and top view (right) of C_{60} nanocolumn array on oxidized Si. (c) Section view (left) and top view (right) of pentacene nanocolumn array on ITO. (d) Section view (left) and top view (right) of pentacene film on ITO in normal incidence.

C_{60} nanocolumn arrays could be realized on both oxidized Si and ITO substrates at a substrate rotation speed of 0.3 rpm. Representative SEM micrographs are depicted in Figs. 2(a) and 2(b). The individual column widths for C_{60} arrays are in the rather narrow range of 70–100 nm. The height of the columns (90 nm) is very uniform. Note that no clear intralayer contrast was observed in SEM images of C_{60} layers prepared on ITO under normal molecular incidence conditions. Figure 2(c) shows an array of pentacene nanocolumns deposited on ITO at the oblique-incidence angle of 80° and a substrate rotation speed of 3 rpm. The diameter of the individual columns in such samples is mainly in the range of 80–120 nm, with a few exceptions reaching ~200 nm. The height of these pentacene columns is rather uniform as well (~360 nm). From the section view (left part) it is apparent that there is no significant variation in column diameter as a function of column height. The top-view image (right part) reveals that pentacene columns appear square shaped. This is an indication that pentacene columns are crystalline, which will be substantiated by x-ray diffraction results presented further below. Details of the interplay between sample preparation parameters (e.g., glancing angle, rotation speed) and obtained morphology will be reported separately.

In contrast, pentacene films deposited onto oxidized Si under the same conditions as used for ITO exhibit very different morphology. A section view (left) and a top view (right) of a pentacene film on an oxidized Si substrate are depicted in Fig. 3(a). There is no columnar structure, and the film morphology resembles closely that, which is typically obtained for pentacene deposited on oxidized Si substrates

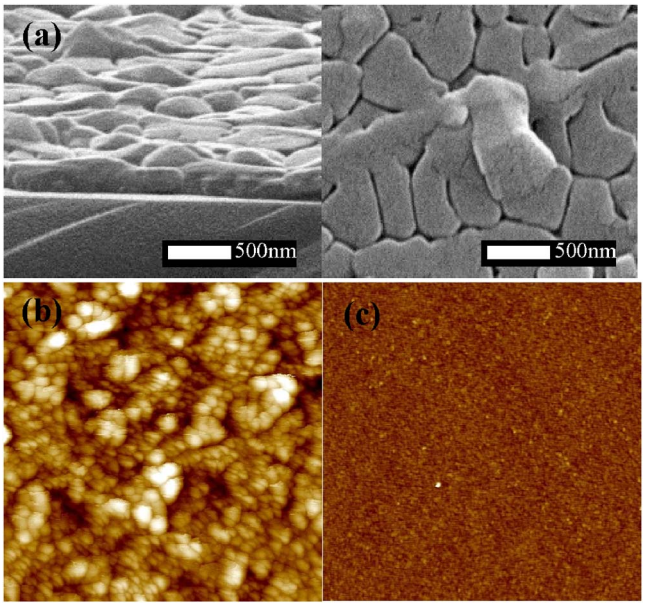

FIG. 3. (Color online) (a) SEM section view (left) and top view (right) micrographs of pentacene/oxidized Si. (b) AFM micrograph of ITO and (c) oxidized Si (both AFM images, 1×1 μm^2; height-scale, 10 nm for ITO and 2 nm for oxidized Si).

with normal molecular flux incidence, i.e., dendritic-shaped islands of micrometer extension.[15] We relate the marked difference in morphology for pentacene on ITO and oxidized Si by GLAD to the molecular surface diffusion length, as outlined in the following. Figures 3(b) and 3(c) display AFM images of the bare ITO and oxidized Si substrates. While the surface roughness of ITO is ~2.3 nm, oxidized Si exhibits a roughness below 0.20 nm. Numerous studies on the growth of pentacene films on oxidized Si by normal-incidence molecular beam deposition have shown that it can be understood in the general framework of diffusion-limited aggregation.[16] On oxidized Si at room temperature, typical molecular diffusion lengths scale with the average size of the islands, which can reach several micrometers for pentacene.[17,18] On the flat oxidized Si, pentacene molecules in GLAD arrive with a significant unidirectional momentum parallel to the substrate surface. However, this directionality can be efficiently randomized during the extended surface diffusion.[14] Therefore, no columnar growth of pentacene on oxidized Si can be initiated by GLAD, and the morphology is essentialy the same as for normal incidence deposition.

On the other hand, the rough ITO surface will seriously limit the diffusion of pentacene molecules.[19] By and large, pentacene molecules will remain on the grain that they initially arrived at, leading to rapid island growth in the direction normal to the substrate surface. Because of the oblique incidence, newly arriving pentacene molecules will be shadowed by neighboring islands.[20] As a result, the observed pentacene nanocolumn array is formed on ITO. Since C_{60} exhibits similar nanocolumns on both substrates, we conclude that the surface diffusion length of C_{60} is comparable on oxidized Si and ITO. Consequently, we propose that the surface diffusion length of molecules on substrates is a critical parameter for the fabrication of organic nanocolumn arrays by GLAD. Apparently, an early onset of three-dimensional island growth is preferred, in order to exploit the shadowing effect by neighboring islands. Future studies will be directed at controlling molecular surface diffusion by chemical sur-

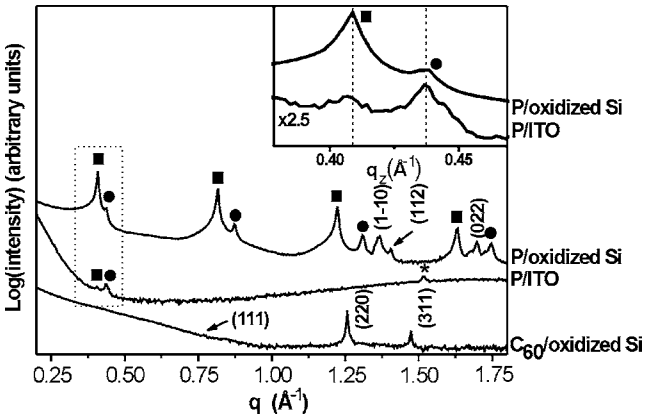

FIG. 4. Specular x-ray diffraction scans of pentacene (P) on oxidized Si (P/oxidized Si) and on ITO (P/ITO), and C_{60} on oxidized Si (C_{60}/oxidized Si) samples prepared by GLAD. The spectrum of a pentacene film on oxidized Si exhibits two series of peaks assigned to the two (00*l*) series of the pentacene thin film phase (squares) and the pentacene bulk phase (circles); the first order peaks (001) of both polymorphs can also be found in the scan of the pentacene nanocolumn array on ITO (inset). The star indicates a diffraction peak from ITO.

face modification and also by substrate patterning.

The square shape of the pentacene nanocolumns on ITO already indicated a crystalline structure. Figure 4 displays x-ray diffraction spectra of pentacene on oxidized Si and on ITO, as well as C_{60} on oxidized Si substrates. For pentacene on oxidized Si, we find two series of peaks denoted with squares and circles, which can be assigned to the 00*l* series of the pentacene thin film phase (squares, measured lattice spacing of $d_{001}=1.541$ nm) and of a recently reported pentacene bulk phase (circles, $d_{001}=1.437$ nm), respectively.[21,22] This preferred orientation of pentacene on oxidized Si is well documented in the literatures. Additionally, less intense peaks can be assigned to crystal planes of another different pentacene polymorph[23] [marked with the respective indices (*hkl*) in Fig. 4]. Most notably, the (001) peaks of the two polymorphs can also be found in the spectrum of the pentacene nanocolumn array on ITO (magnified in the inset of Fig. 4). Interestingly, the relative abundance of the two polymorphs is different for the two substrates, which may be related to different growth dynamics on ITO brought about by the lateral diffusion limitation on this rough surface (see discussion above). Finally, also for C_{60} nanocolumns on oxidized Si, we find a series of peaks, which can be assigned to a cubic polymorph of C_{60} with a lattice constant of 1.415 nm.[24,25] Therefore, in all three cases crystalline organic nanostructures were obtained.

In conclusion, crystalline nanocolumn arrays of two organic semiconductors (pentacene and C_{60}) were fabricated by GLAD and characterized by SEM and x-ray diffraction. For both materials, column diameters of typically 100 nm were found on the transparent conductive oxide ITO. On oxidized Si only C_{60} formed nanocolumns, while pentacene exhibited a morphology resembling that obtained by regular normal incidence deposition. The molecular surface diffusion length on the substrate is identified as critical parameter for the formation of columnar nanostructures by GLAD. With this knowledge, this deposition technique can be easily generalized for the fabrication of organic crystalline nanocolumnar arrays on technologically relevant substrates.

This work was supported by the Sfb448 (DFG). J.Z. acknowledges the Alexander von Humboldt Foundation for an individual research fellowship. N.K. acknowledges financial support by the Emmy Noether-Program (DFG).

[1] M. H. Huang, S. Mao, H. Feick, H. Yan, Y. Wu, H. Kind, E. Weber, R. Russo, and P. D. Yang, Science **292**, 1897 (2001).
[2] X. J. Tang, G. Zhang, and Y. P. Zhao, Nanotechnology **17**, 4439 (2006).
[3] Y. Kawakami, S. Suzuki, A. Kaneta, M. Funato, A. Kikuchi, and K. Kishino, Appl. Phys. Lett. **89**, 163124 (2006).
[4] Z. F. Ren, Z. P. Huang, W. J. Xu, J. H. Wang, P. Bush, M. P. Siegal, and P. N. Provencio, Science **282**, 1105 (1998).
[5] S. S. Fan, M. G. Chapline, N. R. Franklin, T. W. Tombler, A. M. Cassell, and H. J. Dai, Science **283**, 512 (1999).
[6] P. C. P. Hrudey, B. Szeto, and M. J. Brett, Appl. Phys. Lett. **88**, 251106 (2006).
[7] P. C. P. Hrudey, K. L. Westra, and M. J. Brett, Adv. Mater. (Weinheim, Ger.) **18**, 224 (2006).
[8] F. Yang, M. Shtein, and S. R. Forrest, Nat. Mater. **4**, 37 (2005).
[9] V. M. Burlakov, G. A. D. Briggs, and A. P. Sutton, Mater. Res. Soc. Symp. Proc. **708**, BB10.41 (2002).
[10] N. O. Young and J. Kowal, Nature (London) **183**, 104 (1959).
[11] K. Robbie, M. J. Brett, and A. Lakhtakia, Nature (London) **384**, 616 (1996).
[12] K. Robbie and M. J. Brett, J. Vac. Sci. Technol. A **15**, 1460 (1997).
[13] Y. P. Zhao, D. X. Ye, G. C. Wang, and T. M. Lu, Nano Lett. **2**, 351 (2002).
[14] L. Abelmann and C. Lodder, Thin Solid Films **305**, 1 (1997).
[15] R. Ruiz, D. Choudhary, B. Nickel, T. Toccoli, K. Chang, A. C. Mayer, P. Clancy, J. M. Blakely, R. L. Headrick, S. Iannotta, and G. G. Malliaras, Chem. Mater. **16**, 4497 (2004).
[16] F. J. M. Heringdorf, M. C. Reuter, and R. M. Tromp, Nature (London) **412**, 517 (2001).
[17] R. Ruiz, B. Nickel, N. Koch, L. C. Feldman, R. F. Haglund, A. Kahn, F. Family, and G. Scoles, Phys. Rev. Lett. **91**, 136102 (2003).
[18] R. Ruiz, B. A. Nickel, N. Koch, G. Scoles, L. C. Feldman, R. F. Haglund, and A. Kahn, Phys. Rev. B **67**, 125406 (2003).
[19] S. Steudel, S. D. Vusser, S. D. Jonge, D. Janssen, S. Verlaak, J. Genoe, and P. Heremans, Appl. Phys. Lett. **85**, 4400 (2004).
[20] In fact, we can exclude nanocolumn array growth when using normal incidence geometry, as in this case a laterally fully closed pentacene layer is formed [Fig. 2(d)].
[21] C. Mattheus, G. Wijs, R. Groot, and T. Palstra, J. Am. Chem. Soc. **125**, 6323 (2003).
[22] C. C. Mattheus, A. B. Dros, J. Baas, A. J. Meetsma, L. Boer, and T. T. M. Palstra, Acta Crystallogr., Sect. C: Cryst. Struct. Commun. **57**, 939 (2001).
[23] Cambridge Structural Database (CSD) reference code PENCEN03.
[24] D. Andre, A. Dworkin, H. Szwarc, R. Ceolin, V. Agafonov, C. Fabre, A. Rassat, L. Straver, P. Bernier, and A. Zahab, Mol. Phys. **76**, 1311 (1992).
[25] C. F. Macrae, P. R. Edgington, P. McCabe, E. Pidcock, G. P. Shields, R. Taylor, M. Towler, and J. J. Streek, J. Appl. Crystallogr. **39**, 453 (2006).